Journal of King Saud University - Science 36 (2024) 103336

HOSTED BY

Contents lists available at ScienceDirect

Journal of King Saud University - Science

journal homepage: www.sciencedirect.com

Biosynthesis, characterization and monitoring *in vitro* antibacterial efficiencies of AgNPs with filamentous cyanobacteria *Spirulina* sp. And *S. Subsalsa* against pathogenic bacteria

Shuvasree Bej [a], Surendra Swain [a], Ajit Kumar Bishoyi [a,b], Chita Ranjan Sahoo [a], Bigyan Ranjan Jali [c], Mohd Shahnawaz Khan [d], Rabindra Nath Padhy [a,*]

[a] *Central Research Laboratory, IMS & Sum Hospital, Siksha O Anusandhan Deemed to be University, Kalinga Nagar, Bhubaneswar 751003, Odisha India*
[b] *Department of Clinical Hematology, Institute of Medical Sciences & Sum Hospital, Siksha 'O' Anusandhan Deemed to be University, Bhubaneswar, Odisha 751003, India*
[c] *Department of Chemistry, Veer Surendra Sai University of Technology Burla Sambalpur Odisha, 768018 India*
[d] *Department of Biochemistry, College of Science, King Saud University, Riyadh 11451, Saudi Arabia*

ARTICLE INFO

Keywords:
Cyanobacteria
Biosynthesis
Silver nanoparticle
Characterization
Antibacterial efficiency

ABSTRACT

Silver nanoparticles are a fascinating nanomaterial group among metallic nanoparticles for several possible uses, mainly for controlling multidrug-resistant human pathogenic bacteria. The objectives here are to focus on the characterization and observation of antibacterial efficacies of AgNPs biosynthesized using the aqueous extracts of two filamentous non-nitrogen fixing cyanobacteria, *Spirulina* sp. and *Spirulina subsalsa* against bacteria. Characterizations of biosynthesized AgNPs with ultraviolet–visible spectroscopy, field emission scanning electron microscopy, Fourier transform infrared spectroscopy, dynamic light scattering, and X-ray diffraction analysis were done. The ultraviolet–visible spectrum demonstrated the reduction of *S. subsalsa*-AgNPs with a plasmon resonance peak of 458 nm and *Spirulina* sp.-AgNPs with a peak value of 432 nm, indicative of the yield of biosynthesized AgNPs. The antibacterial efficiencies were observed against MDR strains isolated from clinical samples of this hospital with Gram-negative bacteria, *Escherichia coli* (MTCC443), *Acinetobacter baumannii* (MTCC1425), and Gram-positive bacterium, *Streptococcus pyogenes* (MTCC1982) by the agar-well diffusion method. The minimum inhibitory concentration was 50–100 μg/ml, and the minimum bactericidal concentration value was 80–140 μg/ml in both *Spirulina* species. The synthesized AgNPs were more potent during *in vitro* control of MDR h-pathogenic bacteria with the zones of inhibitions at 14 and 15 mm for *Spirulina* sp.-AgNPs. and 15, 14, and 13 mm for *S. subsalsa*-AgNPs. Additionally, FESEM images were used to analyze spherical surface morphology with sizes ranging from 40 to 50 μm. The novelty of the study highlights the biosynthesis of AgNPs individually with *S. subsalsa* and *Spirulina* sp.; eventually, each cyanobacterial biomass holds some great promise for antimicrobial use against h-pathogenic MDR bacteria. Furthermore, research signifies the AgNP biosynthesis with cyanobacteria, evaluates the biocompatibility, and check for host-toxicities of the biosynthesized AgNPs for future possible therapeutic applications.

Abbreviations: AgNPs, Silver nanoparticles; DLS, Dynamic light scattering; DPPH, Diphenyl picrylhydrazyl; FESEM, Field emission scanning electron microscopy; FRAP, Ferric reducing/ antioxidant power; FTIR, Fourier transform infrared spectroscopy; GLA, Gamma-linoleic acid; MBC, Minimum bactericidal concentrations; MDR, Multidrug-resistant; MHA, Mueller-Hinton Agar; MHB, Mueller Hinton Broth; MIC, Minimum inhibitory concentration; NPs, Nanoparticles; PBPs, Phycobiliproteins; PDI, Polydispersity index; ROS, Reductive oxygen species; SPR, surface plasmon variation; *Ss*-AgNPs, *Spirulina subsalsa*-AgNPs; *S*sp-AgNPs, *Spirulina* sp.-AgNPs; UV–Vis, Ultraviolet–visible spectroscopy; XRD, X-ray diffraction analysis; ZOI, Zone of inhibition.

* Corresponding author at: Central Research Laboratory, Institute of Medical Sciences, Siksha 'O' Anusandhan Deemed to be University, Bhubaneswar 751003, Odisha, India.
E-mail address: rnpadhy54@gmail.com (R.N. Padhy).

https://doi.org/10.1016/j.jksus.2024.103336
Received 15 April 2024; Received in revised form 25 June 2024; Accepted 2 July 2024
Available online 2 July 2024

1. Introduction

Due to inherent distinct qualities, such as high surface area, reactivity and durability, silver nanoparticles (AgNPs) have become popular as antimicrobial agents. Antibacterial overuses, which concomitantly lead to bacterial resistance have made antibiotics obsolete and/ or less efficient over the past decades; nevertheless, several tactics such as chemical modifications of the obsolete drug and administration of an antibiotic member of a higher generation or combinatorial therapy could be employed to counteract critical clinical problems. Amino acids and DNA interact in the biosynthesis of AgNPs from broken cell proteins, aiding in possible druggable use as antibacterials (Shantkriti et al., 2023). Particularly, compared to conventional physicochemical methods, the synthesis of AgNPs using biological systems offers several advantages, such as the ability to control the size and form of the particles and less negative environmental impacts without any use of external energy. In contrast to expensive and hazardous physicochemical synthesis techniques, biologically generated AgNPs have solubility in water, and yields. Moreover, these techniques produce nanoparticles (NPs) that are bound to health-sensitive substances, which eventually compromise their application in medicine (Zahin et al., 2020). An easy one-step method can be utilized to create biosynthesis of AgNPs using plant extracts, with examples, the dried root of *Zingiber officinale* (Vijaya et al., (2017), aqueous leaf extracts of *Passiflora edulis f. flavicarpa* (Thomas et al., 2019), *Basella alba* leaf (Mani et al., 2021), and using *Aspalathus* linearis leaf extract by α-$Ni(OH)_2$ (Diallo et al., 2018) for semiconductor metal oxide nanocrystals via photocatalytic application, which could generate health-sensitive chemicals (Jahangir et al., 2023). Thus, developing host-safe, NP-processing methods with organisms is coveted (Bhatt et al., 2022).

As it is, marine algae synthesis of NPs is done, and those have antibacterial characteristics (Al Nadhari et al., 2021). Currently, the focus is on locating and evaluating more contemporary natural sources as antioxidants in algae. Algal antioxidant qualities are due to phytochemicals that can be crucial and have high redox potentials (Ismail et al., 2021). For example, cyanobacterial phycobiliproteins (PBPs), namely, C-phycocyanin are abundant as the unique pigments employed by cyanobacteria for oxygenic photosynthesis, which explains oxygenation of the nascent earth; oxygenation could be the bold reaction in waiving out reductive oxygen species (ROS) from tissues suffering from ROS; at body metabolism how, NPs might lessen and stabilize the developing cell, as shown (Kannaujiya et al., 2020). Several tests proved the antioxidant activities of AgNPs, the ferric reducing/ antioxidant power (FRAP) assay, metal chelating activity, superoxide radical scavenging activity, and 2,2-diphenylpicrylhydrazyl (DPPH) radical scavenging activity, etc. (Prajapati et al., 2022). Herein, the green synthesis and monitoring of the antibacterial activities of the biosynthesized AgNPs for their plausible health advantages since both cyanobacterial species used have vitamins, minerals, and vital amino acids (Sharma and Phutela, 2023). Indeed, *Spirulina* sp. and *S. subsalsa* are photosynthetic and spiral, or coiled filamentous cyanobacteria in morphology belonging to the order Oscillatoriales and with pharmaceutics. Because of the high gamma-linoleic acid (GLA) content, Spirulina is a good dietary supplement (Matufi and Choopani, 2020). Various *Spirulina* strains have various lipid and fatty acid compositions, which may also depend on the conditions under which they are cultivated (Lupatini et al., 2017). This study evaluates the biosynthesis of AgNPs with the extract of *Spirulina* sp. and *S. subsalsa* were characterized and their antibacterial efficacies were examined *in vitro*.

2. Materials and methods

2.1. Unialgal biomass production and optimization

Spirulina sp. (strain no. BDU51381) (*Ssp*) and *S. subsalsa* (strain no. BDU101022) (*Ss*) were obtained from Bharathidasan University, Tiruchirappalli, TN, India; and those two taxa were mass-cultured in ASN III medium in a culture room. Individual biomasses were shade-dried for a month at room temperature. The obtained powders were stored in airtight containers. The extracts of *Ssp* and *Ss* were individually combined and incubated for one hour at 90 °C with 2 gm of shade-dried cyanobacterial biomass in 100 ml of deionized water for aqueous extracts to get aqueous extracts. Each extract was filtered to produce a clear solution, and each extract was combined individually with ethanol, methanol, butanol, acetone, and water separately to prepare each alga for antibacterial monitoring (Fig. 1).

2.2. Biosynthesis of AgNPs of Spirulina sp. (Ssp-AgNPs) and S. Subsalsa (Ss-AgNPs)

Two lots of 10 mg of dried biomass of *Ssp* and *Ss* separately were roughly mixed at 40° C for 24 hrs (Sahoo et al., 2020). An aliquot of one milliliter of $AgNO_3$ in a 1 mM solution was added to the aqueous medium. The reaction color was monitored every hour for 48 hrs. When the color of the incubated mixture changed from pale green to deep brown, the lot was repeatedly centrifuged at 4,000 rpm for 10 min (Sahoo et al., 2020). After centrifuging the mixture with AgNPs for 10 min., the individual final pellets were dried at 40° C for ultraviolet–visible spectroscopy (UV–vis), field emission scanning electron microscopy (FESEM), Fourier transform infrared spectroscopy (FT-IR), dynamic light scattering (DLS), and X-ray diffraction analysis (XRD), spectral characterizations. The visible colour change was verified by UV–visible spectrophotometry, which obtained spectral readings at 432 nm and 458 nm for *Ssp*-AgNPs and *Ss*-AgNPs, respectively.

2.3. Spectral characterization by standardization of suitable analytical tools

2.3.1. UV–Vis

The adsorption of each derived tan solution was evaluated using a spectrophotometer (JASCO V-670 UV–VIS-NIR Spectrophotometer; Tokyo, Japan). UV–vis spectra were used to identify the synthesis of silver nanoparticles. The sample was extracted in 0.2 ml aliquots of the colloidal suspension diluted to 2 ml with deionized water. The appearance of a plasmon resonance peak indicated the biogenesis of AgNPs (Zaheer et al., 2023).

2.3.2. FE-SEM

Every sample was photographed at different magnifications, and investigations were conducted into the distribution of particle sizes, presence, aggregation, and density. The morphologies of the nanoparticles, which range from spherical to more complex geometries, may be observed in detail using the great spatial resolution of FESEM, providing insight into their synthesis and stabilization processes. Furthermore, AgNP interactions with bacterial cells are clarified by FESEM, which also helps to understand the mechanisms behind the nanoparticles' antibacterial activity (Bhuyar et al., 2020).

2.3.3. FT-IR

For a Fourier transformer infrared (FTIR), JASCO FT/IR4600-ATR spectrophotometer, at the range of 400–4,000 cm^{-1} was used to identify the functional groups that were thought to be responsible for the reduction of silver ions in the extracts of *Spirulina* sp. and *S. subsalsa*. (Gnanakani et al., 2019).

2.3.4. DLS

The polydispersity index (PDI), hydrodynamic size (Z average), and particle size distribution of NPs were investigated using a DLS method by the MALVERN instrument (ZEN 1600). The size distribution and stability of AgNPs in solution are revealed by DLS, which measures the changes in light scattering caused by the Brownian motion of the nanoparticles. This approach is effective for monitoring size changes

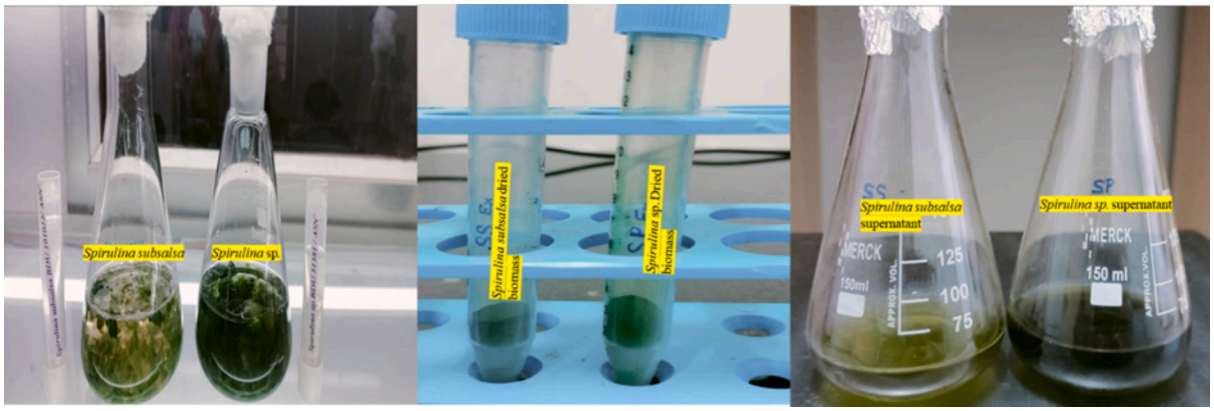

Fig. 1. Experimental setup and biomass production of *S*sp and *Ss* extracts.

over time and assessing the homogeneity of suspensions of nanoparticles (Patil and Chougale, 2021).

2.3.5. XRD

X-ray diffraction was used to analyze the crystal structure of AgNPs, with information on the phase composition, crystallite size, and lattice parameters of the synthesized particles. Following drying, a glass substrate was coated with NP powder and then scanned in the 2θ area at 0.5°/min. Based on the line width of the maximum intensity reflection peak in the XRD pattern and Scherrer's equation, the mean particle diameter of AgNPs was determined (Jebril et al., 2020).

2.4. Applications of biosynthesized AgNPs

2.4.1. Antibacterial activities of Ssp-AgNPs & Ss-AgNPs

The Gram-positive bacterial strain, *Streptococcus pyogenes* (*S. pyogenes*), and the Gram-negative, *Acinetobacter baumannii* (*A. baumannii*), *Escherichia coli* (*E coli*) were cultivated on nutrient, Mueller-Hinton Agar (MHA) and in Mueller Hinton Broth (MHB). Before being maintained in a lab environment at 8 °C for the antibacterial experiment, the bacteria were grown in Mueller Hinton broth (MHB). After isolating one microbe into an aliquot, it was placed in a sterile 15 ml centrifuge tube with a laminar air-flow chamber and 5 ml of nutrient broth (Himedia, M002) medium. Once isolated from clinical samples, these pathogenic bacteria were regrown in laboratory conditions. The MDR strains of *E. coli, A. baumannii,* and *S. pyogenes* were considered for antibacterial activities of the study had previously been identified (Dubey and Padhy, 2013; Rath and Padhy, 2015, Swain et al., 2024).). The isolated bacteria were subjected to antibiotic-susceptibility tests, as described, as signposted: *E. coli* (MTCC443), *A. baumannii* (MTCC1425), and *S. pyogenes* (MTCC1982). MHA plates were used to store the pure bacterial cultures. The microbial strains were swabbed onto MHA plates. The media was stabbed with a sterile puncher to create the 8 mm diameter wells. The positive control was gentamycin. Additionally, a micropipette was used to add 50 µl of the extract to each well. MDR strains of the reported bacteria were used for monitoring biosynthesised nanoparticles' antibacterial efficacies by the agar-well diffusion test and the determination of MICs and MBCs using a 96-well plate and the conventional serial dilution method. Using a standard scale, the inhibitory zone surrounding the dropping was measured in mm. The OD_{600} of each bacterial strain was also used to determine its vitality, which was used to monitor the anti-microbial qualities of AgNPs.

3. Results

3.1. Biosynthesis of AgNPs

Additionally, a color reaction was observed, whereby the transparent $AgNO_3$ solution took on a reddish-brown color, suggesting that silver nanoparticles may eventually surface, as illustrated (Fig. 2). The appearance of a brown color upon visual inspection indicated that *S*sp and *Ss* were utilized in the synthesis of AgNPs.

3.2. Characterizations

3.2.1. Uv–vis spectroscopy of biosynthesized Ssp-AgNPs and Ss-AgNPs

Using UV–visible spectroscopy, *Spirulina* sp., and *S. subsalsa* produced AgNPs with a distinct reddish-brown color (Fig. 2), surface plasmon variation (SPR) caused the color shift, and a prominent peak was seen at 432 and 458 nm in the spectral spectrum of *S*sp. and *Ss* respectively (Fig. 3). SPR in the 450–500 nm spectral band is indicated for optical filtering applications in Ag–TiO_2 nano cermet thin films formed by two different sputtering techniques, as the smaller silver grains spread out from the first heterogeneous layer produced the massive, flat Ag grains that make up the overlayer. The weak SPR absorption at about 700 nm is caused by these anisotropic granules (Dakka et al., 2000). It was in line with previous research, which indicated that the usual SPR peak of AgNPs was located between 440 and 450 nm (Dar et al., 2013). ZnO nanoparticles that have been biosynthesized have been effectively produced utilizing *Moringa oleifera* extract and have been characterized by several approaches. After annealing, pure, single-phase absorbance profiles with a fall beginning at 350 nm and an inflection point at 380 nm, which is equivalent to 3.2 eV and in good agreement with the bandgap of ZnO, are obtained (Matinise et al., 2017). $ZnSnO_3$-NPs were shown to have UV–visible diffused reflectance, an absorption edge at 354 nm, a band gap of 3.50 eV, and possible photocatalytic activity using *Aspalathus linearis* natural extracts (Mayedwa et al., 2018a), and another study revealed a peak of SPR of AgNPs was noted the range of 420 nm (Bishoyi et al., 2021).

3.2.2. FE-SEM of biosynthesized Ssp-AgNPs, and Ss-AgNPs

The morphology of the nanoparticles was assessed by FESEM analysis (Fig. 4). The smaller particles in the FESEM investigation had aggregated to form a larger particle-like appearance. As revealed by SEM investigation, the dispersion of silver nanoparticles on the surface grid amply illustrates the morphological regularity. SEM tests indicated that the *O. princeps* extract generated spherical AgNP units with diameters ranging from 100–200 nm during the manufacture of *O. princeps*-AgNPs (Bishoyi et al., 2021). The synthetic *Spirulina*-AgNPs used in this investigation had a quasi-spherical form and ranged in size from 40-50 µm.

3.2.3. FT-IR spectrometric profile of biosynthesized Ssp-AgNPs and Ss-AgNPs

Spirulina sp. and *S. subsalsa* exhibit distinct peaks at 3332, 1636, and 536 cm^{-1} and 1634, 1634, and 536 cm^{-1}, respectively, FTIR spectra

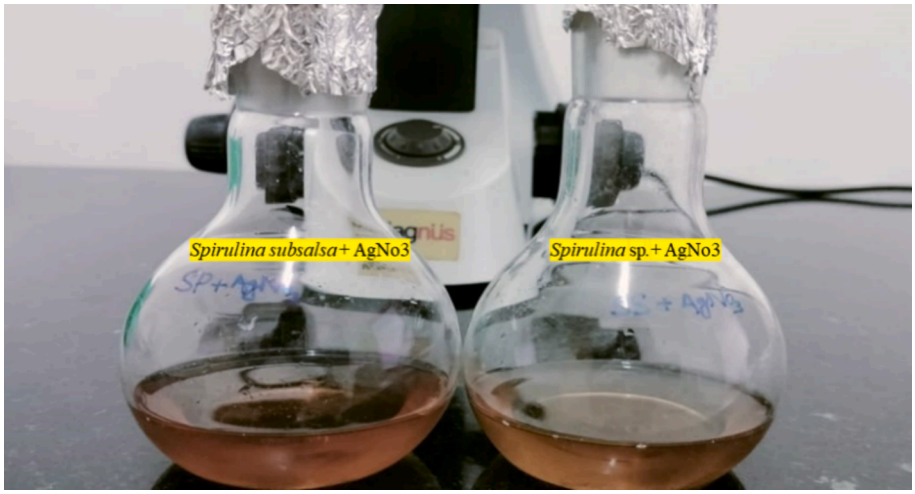

Fig. 2. Formation of color changed after the biosynthesis of *Ss*-AgNPs and *S*sp-AgNPs.

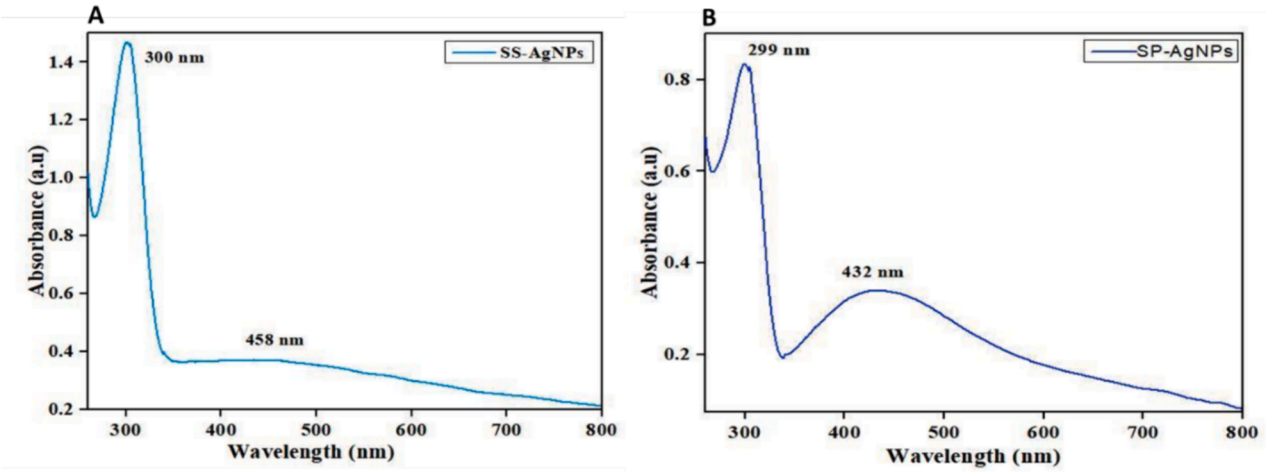

Fig. 3. Observation of SPR absorbance peaks of (A) *Ss*- AgNPs and (B) *S*sp.-AgNPs by UV–vis spectroscopy analysis.

(Fig. 5, Table 1). The *Spirulina* sp. and *S. subsalsa* peaks, respectively, correspond to the N–H group of amino acids at 3350 and 3332 cm^{-1}. One can observe a diketone group as a peak at 1634 and 1636 cm^{-1}. The halogen compound of C caused the peaks at 536 and 524 cm^{-1}. (Fig. 6).

3.2.4. DLS of biosynthesized Ssp-AgNPs, and Ss-AgNPs

The DLS distribution of *Spirulina* AgNPs size was found to range between 30 and 60 nm, however, the previous results were with an average computed size of 26.57 nm and a maximum mean intensity of 3.02 % found to be consistent with the dispersed light intensity value of 976.11 or the mean intensity value of 16.93 (Bishoyi et al., 2021). Pedalium murex produced biogenic AgNP with an average DLS of 73.14 nm (Bishoyi et al., 2021).

3.2.5. XRD of biosynthesized Ss, and Ssp-AgNPs

Moreover, crystalline structures were generated in 0–70 theta (Θ) ranges individually in both *Spirulina* species, the analysis of this study was presented (Fig. 7), and the peaks list of biosynthesized AgNPs (*Ss*-AgNPs, and *S*sp-AgNPs) indicated the crystal size of NPs showed by XRD analysis (Tables S1, and S2). The previous study of XRD analysis with values of 10.3°, 38.90°, and 63.9°, and verified the production of AgNPs. The synthesized AgNPs were generated at two different temperatures, 39.01°, and 64.72°, according to the crystalline pattern (Bishoyi et al., 2021).

3.2.6. Antibacterial properties of biosynthesized Ssp-AgNPs, and Ss-AgNPs

The produced *S*sp-AgNPs and *Ss*-AgNPs exhibited remarkable antibacterial efficacy against bacterial strains, *E. coli, A. baumannii,* and *S. pyogenes.* The MIC values for the bacterial species were 50–100 μg/ml, the MBC value ranged from 80-140 μg/ml where the ZOI of −ve control was 0 mm, + ve control (Gentamycin) ranged from 17 mm to 19 mm. The ZOI of *Ssp*-AgNPs showed higher potencies of killing MDR bacteria than *Ss*-AgNPs (Table 2, Fig. 8). However, the early study ZOI of *S platensis* extracts ranged from 5 to 45 mm at 200 μl/well. The mean ZOI (30 mm) in the *S. platensis* nanomaterial extract inhibited Gram-positive bacteria with ZOI as given, *Pseudomonas aeruginosa* (12 mm), *Staphylococcus aureus*, *Enterococcus faecalis* (6 mm), and *Klebsiella pneumoniae* (11 mm) (Awadalla et al., 2021).

4. Discussion

Cyanobacteria as microalgae, are highly sought after as naturally occurring sources of bioactive compounds with antibacterial, antiviral, anticancer, antioxidant, and anti-inflammatory qualities. They also yield several interesting compounds with a wide spectrum of biological functions (Hassan et al., 2022). Also, plant extracts, *Aspalathus linearis* with green-synthesized palladium and palladium oxide nanoparticles showed two distinct peaks: a broad peak including flavonoids that was centred around 348.5 nm, and a sharp peak containing the aspalathin component that was centred around 284.5 nm (Ismail et al., 2017). Pant-

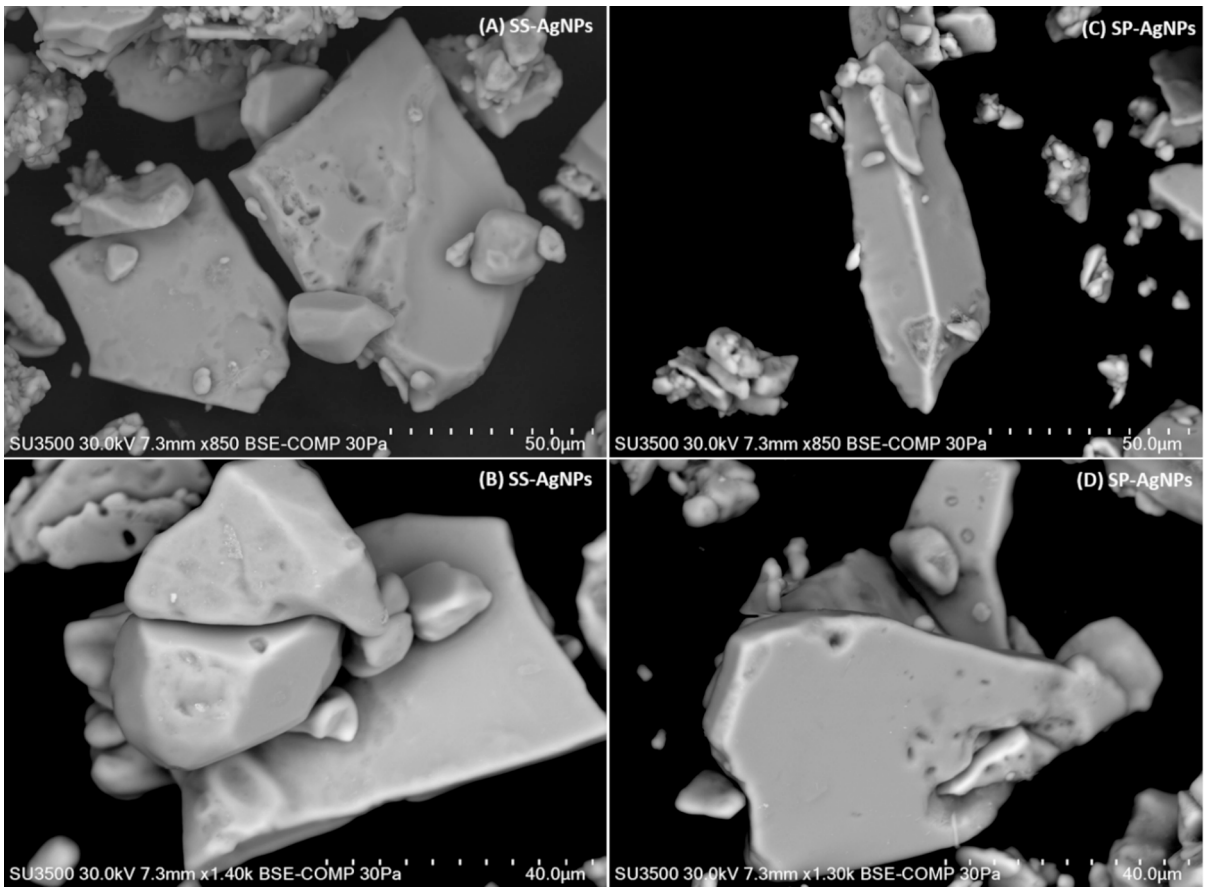

Fig. 4. Observation of size of the particles of *Ss*-AgNPs (A, B), and *S*sp-AgNPs, (C, D) FESEM analysis.

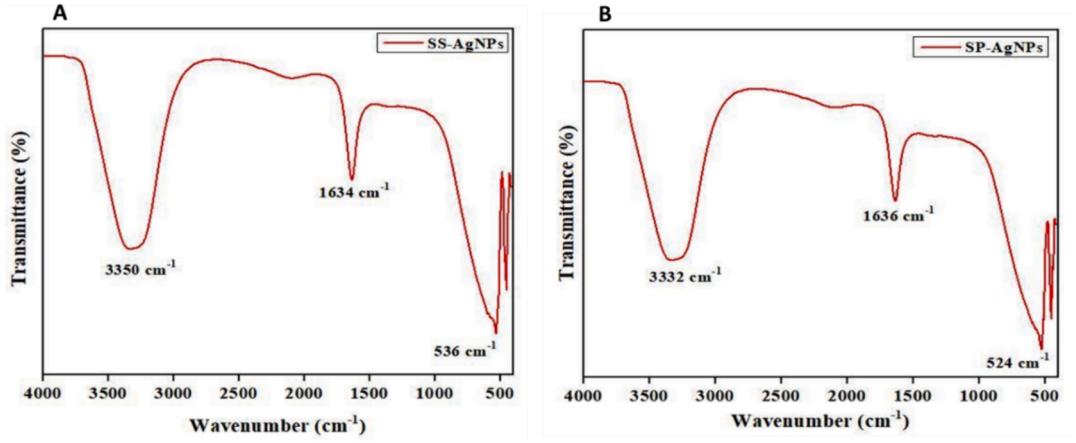

Fig. 5. Observation of peaks of functional groups by FT-IR analysis (A) *Ss*-AgNPs and (B) *S*sp-AgNPs.

Table 1
Peaks of functional groups of *S*sp-AgNPs *and Ss*-AgNPs by FT-IR spectroscopy.

AgNPs	Peak (cm^{-1})	Functional groups
*S*sp- AgNPs	3332	Amino acid (N–H)
	1636	Diketones
	524	Halogen compound (C-I)
Ss- AgNPs	3350	Amino acid (N–H)
	1634	Diketones
	536	Halogen compound (C-I)

mediated green production of NPs of nickel oxide, palladium, and palladium oxide was particularly promising, because *Aspalathus linearis* natural extracts of NPs function as both a capping and reducing agent (Mayedwa et al., 2018b).

Along with the first production and viability of consistently replicating stoichiometric pure textured VO2 nano-structures, a potential vacuum sputtering technique utilizing an inverted cylindrical magnetron to produce nanostructured VO2 thin films was disclosed (Kana Kana et al., 2008). Generally nano system consists of a single dimension that is 100 nm or less, anisotropic, isotropic, and single-dimensional nanoparticles can be produced, in addition to two-dimensional systems like sheets or thin films and multilayered systems like nanocomposites

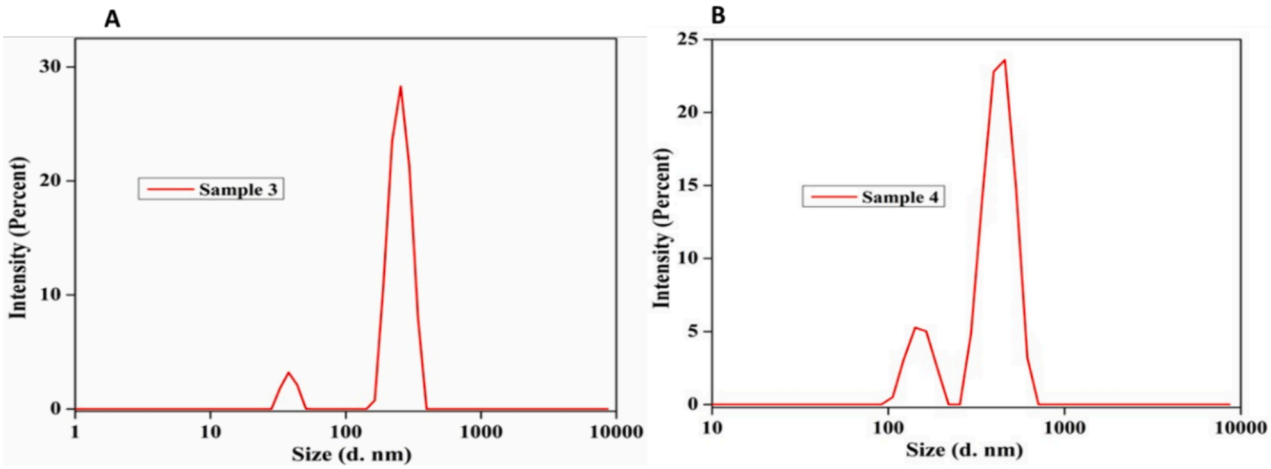

Fig. 6. Observation of size of NPs (A) *Ss*- AgNPs and (B) *S*sp- AgNPs by DLS analysis.

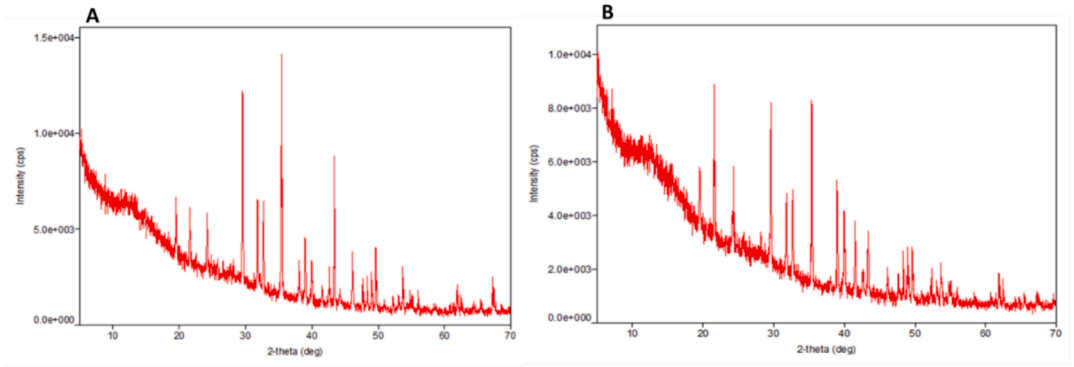

Fig. 7. Observation of crystalline structure of (A) *Ss*- AgNPs and (B) *S*sp- AgNPs by XRD analysis.

Table 2
Antibacterial activities (ZOI, MICs, and MBCs) of biosynthesized *Ssp*-AgNPs and *Ss*-AgNPs against bacteria, *A. baumannii, E. coli,* and *S. pyogenes.*

AgNPs	Bacterium	ZOI of −ve control (mm)	ZOI of + ve control (mm)	ZOI of *S*sp-AgNPs and *Ss*-AgNPs (mm)	MIC (μg/ml)	MBC (μg/ml)
*S*sp-AgNPs	*A. baumannii*	0	19	15	80	100
*S*sp −AgNPs	*E. coli*	0	18	14	50	80
*S*sp −AgNPs	*S. pyogenes*	0	17	14	100	140
Ss-AgNPs	*A. baumannii*	0	18	14	80	120
Ss-AgNPs	*E. coli*	0	18	13	75	130
Ss-AgNPs	*S. pyogenes*	0	17	12	60	90

(Henini et al., 2022).

The nanomaterial had the largest ZOI against *Yersinia pestis*, 45 mm, when compared to an organic solvent extract (Na-citrate) against *Staphylococcus aureus* (ZOI, 20 mm) (Awadalla et al., 2021). Instead of using prescription antimicrobials, *S. platensis* is an affordable antibacterial agent that can be used to combat harmful bacteria. It has been demonstrated that phycobiliproteins isolated from these species have several beneficial health effects, including boosting immune response. These pigments are widely used in the food, pharmaceutical, and cosmetics industries as natural alternatives to artificial colorants. *Spirulina* sp. is filamentous, multicellular, photoautotrophic biomass cyanobacteria resistant to the extreme environments seen in wetlands. It is rich in essential proteins, minerals, vitamins, and fatty acids used in many industries.

The cyanobacteria that produce oxygen share cytological similarities with Gram-negative bacteria, which are recognized for possessing phycobiliproteins in red and blue colors that are soluble in both water and chlorophyll *a*. Because of their chromatic adaptation mechanisms, cyanobacteria can survive in harsh environments with high salinity, low water content, heat, cold, nitrogen deficiency, photo-oxidation, osmotic stress, and ultraviolet light (Yarkent et al., 2020). Several compounds have undergone preclinical and/or clinical testing as possible anticancer medications, including the anti-microtubule medicines dolastatin 10 and curacin A (Barreca et al., 2020).

5. Conclusion

This research describes the characterization of products such as UV–vis spectroscopy results that confirmed the formation of AgNPs, and the FTIR analysis that identified the biomolecules responsible for the stability and reduction of the nanoparticles. XRD analyses were utilized to ascertain the dimensions, shape, and crystalline nature of the generated AgNPs. The significant antibacterial efficacy of AgNPs against bacteria was suggested by the potential application demonstrated by their ZOI, and MICs/MBC indicating the potential utility of medications of innovative antimicrobials. Future research efforts must focus on the *in*

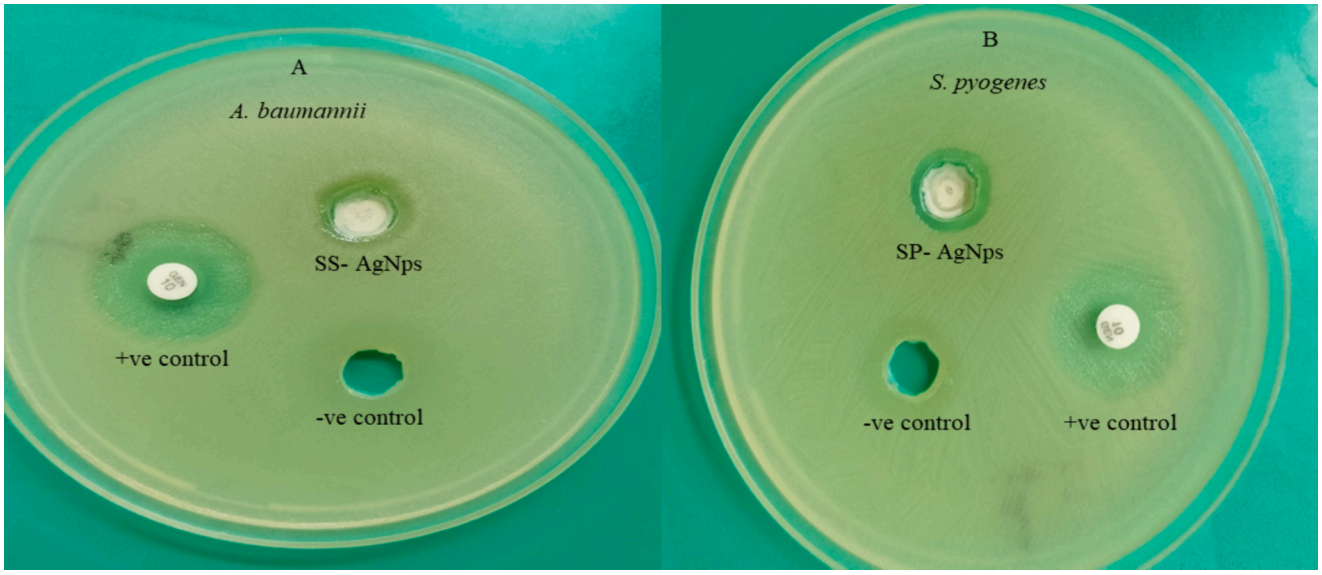

Fig. 8. Observations of antibacterial activity, (A) *Ss-AgNPs* against *A. baumannii*, (B) *Ssp-AgNPs* against *S. pyogenes.*

vitro assessment of these biosynthesized AgNPs and the development of practical applications were successfully synthesized by biological methods and combined with *S. subsalsa* and *Spirulina* sp. extracts. This study has shown the antibacterial activities of synthesized cyanobacterial extracts with $AgNO_3$ against bacteria. A synergistic impact against *E. coli*, *A. baumannii*, and *S. pyogenes* was seen when conjugating AgNPs claimed that all conjugates with effects are responsible for increasing the efficacy of various extracts and conventional antibacterial drugs.

Funding information

MSK acknowledges the generous support from the Research supporting project (RSP2024R352) by King Saud University, Riyadh, Kingdoms of Saudi Arabia. The extramural fund was unavailable; S. Bej, as the Ph.D. research fellow (Regd. no. 218https://doi.org/1002054/2021) and the work was supported by SOA University, Bhubaneswar.

CRediT authorship contribution statement

Shuvasree Bej: Writing – review & editing, Writing – original draft, Validation, Methodology, Investigation, Data curation, Conceptualization. **Surendra Swain:** Writing – review & editing, Visualization, Formal analysis. **Ajit Kumar Bishoyi:** Writing – review & editing, Visualization, Conceptualization. **Chita Ranjan Sahoo:** Writing – review & editing, Visualization, Conceptualization. **Bigyan Ranjan Jali:** Writing – review & editing, Methodology. **Mohd Shahnawaz Khan:** Visualization, Funding acquisition. **Rabindra Nath Padhy:** Writing – review & editing, Visualization, Supervision, Funding acquisition.

Declaration of Competing Interest

The authors declare that they have no known competing financial interests or personal relationships that could have appeared to influence the work reported in this paper.

Acknowledgments

We are grateful to Prof. Dr. S. Mishra, Dean, IMS & Sum Hospital, Bhubaneswar, Shiksha O Anusandhan University, Odisha, for the facilities. S. Bej is grateful to Prof. J. K. Nath, Dean (R & D) of SOA University for the SOA-PhD fellowship, support, and work as part of the Ph.D. thesis. No. 2181002054/2021,We are grateful to MSK(RSP2024R352) for Research supporting.

Appendix A. Supplementary material

Supplementary data to this article can be found online at https://doi.org/10.1016/j.jksus.2024.103336.

References

AlNadhari, S., et al., 2021. A review on biogenic synthesis of metal nanoparticles using marine algae and its applications. Environ. Res. 194–110672 https://doi.org/10.1016/j.envres.2020.110672.

Awadalla, O.A., et al., 2021. Antimicrobial activities of *Spirulina platensis* extracts and nanoparticles material against some pathogenic bacterial isolates. Egypt J. Appl. Sci. 36, 5–6. https://doi.org/10.21608/ejas.2021.183463.

Barreca, M., et al., 2020. An overview on anti-tubulin agents for the treatment of lymphoma patients. Pharmaco & Therape. 211, 107552 https://doi.org/10.1016/j.pharmthera.2020.107552.

Bhatt, P., et al., 2022. Nanobioremediation: A sustainable approach for the removal of toxic pollutants from the environment. J. Hazard. Mater. 427, 128033 https://doi.org/10.1016/j.jhazmat.2021.128033.

Bhuyar, P., et al., 2020. Synthesis of silver nanoparticles using marine macroalgae Padina sp. and its antibacterial activity towards pathogenic bacteria. Beni-Suef Univer J Basic Appl Sci 1–5. https://doi.org/10.1186/s43088-019-0031-y.

Bishoyi, A.K., et al., 2021. Biosynthesis of silver nanoparticles with the brackish water blue-green alga *Oscillatoria princeps* and antibacterial assessment. Appl Nanosci. 389–98 https://doi.org/10.1007/s13204-020-01593-7.

Dakka, A., et al., 2000. Optical properties of Ag–TiO 2 nanocermet films prepared by co-sputtering and multilayer deposition techniques. Applied Optic. 16, 2745–2753. https://doi.org/10.1364/AO.39.002745.

Dar, M.A., et al., 2013. Enhanced antimicrobial activity of silver nanoparticles synthesized by *Cryphonectria* sp. evaluated singly and in combination with antibiotics. Nanomed: Nanotechnol. Bio Medi 1, 105–110.

Diallo, A., et al., 2018. Structural, optical and photocatalytic applications of biosynthesized NiO nanocrystals. Green Chem Lett Revis. 2, 166–175.

Dubey, D., Padhy, R.N., 2013. Antibacterial activity of *Lantana camara* L. against multidrug resistant pathogens from ICU patients of a teaching hospital. J Herb Med. 2, 65–75. https://doi.org/10.1016/j.hermed.2012.12.002.

Gnanakani, P.E., et al., 2019. Nannochloropsis extract–mediated synthesis of biogenic silver nanoparticles, characterization and in vitro assessment of antimicrobial, antioxidant and cytotoxic activities. Asia Pacif. J. Cancer Preven. 8, 2353.

Hassan, S., et al., 2022. Identification and characterization of the novel bioactive compounds from microalgae and cyanobacteria for pharmaceutical and nutraceutical applications. J. Basic Microbiol. 9, 999–1029.

Henini, M., et al., 2022. Peculiar size effects in nanoscaled systems. Nano-Horizons. 1, 1. https://doi.org/10.25159/Nano Horizons.9d53e2220e31.

Ismail, E., et al., 2017. Green palladium and palladium oxide nanoparticles synthesized via *Aspalathus linearis* natural extract. J Alloys Compound. 695, 3632–3638. https://doi.org/10.1016/j.jallcom.2016.11.390.

Ismail, G.A., et al., 2021. Antimicrobial, antioxidant, and antiviral activities of biosynthesized silver nanoparticles by phycobiliprotein crude extract of the cyanobacteria *Spirulina platensis* and *Nostoc linckia*. Bionanosci. 11, 355–370. https://doi.org/10.1007/s12668-021-00828-3.

Jahangir, R., et al., 2023. One-step synthesis of ultrasmall nanoparticles in glycerol as a promising green solvent at room temperature using omega-shaped microfluidic micromixers. Anal. Chem. 4, 1–20. https://doi.org/10.1021/acs.analchem.3c01697.

Jebril, S., et al., 2020. Green synthesis of silver nanoparticles using *Melia azedarach* leaf extract and their antifungal activities: *In vitro* and *in vivo*. Mater Chem Phy. 248, 122898 https://doi.org/10.1016/j.matchemphys.2020.122898.

Kannaujiya, VK., et al., 2020. Phycobiliproteins in microalgae: Occurrence, distribution, and biosynthesis. Pigment from microalgae handbook. p43-68. Doi: 10.1007/978-3-030-50971-2_3.

Lupatini, A.L., et al., 2017. Potential application of microalga *Spirulina platensis* as a protein source. J. Sci. Food Agri. 3, 724–732. https://doi.org/10.1002/jsfa.7987.

Mani, M., et al., 2021. Studies on the spectrometric analysis of metallic silver nanoparticles (AgNPs) using *Basella alba* leaf for the antibacterial activities. Environ. Res. 199, 111274 https://doi.org/10.1016/j.envres.2021.111274.

Matinise, N., et al., 2017. ZnO nanoparticles via *Moringa oleifera* green synthesis: physical properties & mechanism of formation. Appl. Surf. Sci. 406, 339–347. https://doi.org/10.1016/j.apsusc.2017.01.219.

Matufi, F., Choopani, A., 2020. *Spirulina*, food of past, present and future. HealthBiotechnol Biopharm. 3, 1–20.

Mayedwa, N., et al., 2018a. Green synthesis of zin tin oxide (ZnSnO3) nanoparticles using *Aspalathus linearis* natural extracts: Structural, morphological, optical and electrochemistry study. Appl. Surf. Sci. 446, 250–257. https://doi.org/10.1016/j.apsusc.2017.12.161.

Mayedwa, N., et al., 2018b. Green synthesis of nickel oxide, palladium and palladium oxide synthesized via *Aspalathus linearis* natural extracts: physical properties and mechanism of formation. Appl. Surf. Sci. 446, 266–272. https://doi.org/10.1016/j.apsusc.2017.12.116.

Patil, R.B., Chougale, A.D., 2021. Analytical methods for the identification and characterization of silver nanoparticles: a brief review. Mater Today: Proceed. 47, 5520–5532. https://doi.org/10.1016/j.matpr.2021.03.384.

Prajapati, S.K., et al., 2022. Nanodelivery of antioxidant herbal extracts, spices, and dietary constituents. Phytoantiox Nanotherap. 12, 145–171. https://doi.org/10.1002/9781119811794.ch8.

Rath, S., Padhy, R.N., 2015. Antibacterial efficacy of five medicinal plants against multidrug-resistant enteropathogenic bacteria infecting under-5 hospitalized children. J. Integr. Med. 1, 45–57. https://doi.org/10.1016/S2095-4964(15)60154-6.

Sahoo, C.R., et al., 2020. Biogenic silver nanoparticle synthesis with cyanobacterium *Chroococcus minutus* isolated from Baliharachandi sea-mouth, Odisha, and *in vitro* antibacterial activity. Saud. J. Bio. Sci. 6, 1580–1586. https://doi.org/10.1016/j.sjbs.2020.03.020.

Shantkriti, S., et al., 2023. Biosynthesis of silver nanoparticles using *Dunaliella salina* and its antibacterial applications. Appl. Surf. Sci. Adv. 100377, 1–13. https://doi.org/10.1016/j.apsadv.2023.100377.

Sharma, N., Phutela, U.G., 2023. Analysis of the growth profile, biochemical composition and nutrient removal efficacy of *Spirulina* sp. NCIM 5143. Environ.Conser J. 24, 269–286. https://orcid.org/0000-0001-8026-0125.

Swain, S., et al., 2024. Biosynthesis and characterizations of silver nanoparticles with filamentous cyanobacterium *Lyngbya* sp. with *in vitro* antibacterial properties against MDR pathogenic bacteria. Naunyn-Schmiedeberg's Archiv Pharmacol. Doi: 10.1007/s00210-024-03235-z.

Thomas, B., et al., 2019. Antioxidant and photocatalytic activity of aqueous leaf extract mediated green synthesis of silver nanoparticles using *Passiflora edulis f. flavicarpa*. J. Nanosci. Nanotechnol. 5, 2640–2648. https://doi.org/10.1166/jnn.2019.16025.

Vijaya, J.J., et al., 2017. Bioreduction potentials of dried root of *Zingiber officinale* for a simple green synthesis of silver nanoparticles: antibacterial studies. J. Photo. Photo. Biol. 177, 62–68. https://doi.org/10.1016/j.jphotobiol.2017.10.007.

Yarkent, Ç., et al., 2020. Potential of microalgal compounds in trending natural cosmetics: a review. Sustain. Chem. Pharmac. 17, 100304 https://doi.org/10.1016/j.scp.2020.100304.

Zaheer, Z., et al., 2023. Effects of anionic and cationic surfactants on the surface Plasmon resonance intensity of biogenic silver nanoparticles: stability, and position of optical band. J. Mol. Liq. 385, 122363 https://doi.org/10.1016/j.molliq.2023.122363.

Zahin, N., et al., 2020. Nanoparticles and its biomedical applications in health and diseases: special focus on drug delivery. Environ. Sci. Pollut. Res. 68, 19151 https://doi.org/10.1007/s11356-019-05211-0.